STRUCTURE AND INFRASTRUCTURE ENGINEERING, 2016
VOL. 12, NO. 9, 1202–1215
http://dx.doi.org/10.1080/15732479.2015.1099110

Taylor & Francis
Taylor & Francis Group

On the accuracy of diffusion models for life-cycle assessment of concrete structures

Andrea Titi and Fabio Biondini

Department of Civil and Environmental Engineering, Politecnico di Milano, Milan, Italy

ABSTRACT

In durability analysis and life-cycle assessment of concrete structures transport of chlorides and other aggressive agents is generally described by using Fick's laws of diffusion. This model is frequently applied in a simplified one-dimensional (1D) form. However, in practical applications the diffusion process is more properly described by two- or three-dimensional patterns of concentration gradients. In this paper, the accuracy of the 1D modelling of diffusion and its impact on the life-cycle assessment of concrete structures under corrosion is evaluated in deterministic and probabilistic terms with respect to more accurate two-dimensional (2D) formulations. The influence of the diffusion modelling on the time-variant corrosion damage of concrete cross-sections is studied with reference to the local damage of the reinforcing steel bars and the global deterioration of bending moment–curvature capacity curves. The results show that 2D diffusion models may be necessary for a realistic life-cycle assessment of concrete structures under corrosion, since 1D models can lead to significant inaccuracies depending on the geometrical aspect ratio of the cross-section, location of reinforcing steel bars and exposure conditions.

ARTICLE HISTORY
Received 12 March 2015
Revised 4 August 2015
Accepted 15 September 2015
Published Online 24 December 2015

KEYWORDS
Concrete structures; durability; corrosion; life-cycle assessment; diffusion models; cellular automata

Introduction

Due to ageing and environmental aggressiveness, concrete structures are subjected to a progressive deterioration which may lead over time to unsatisfactory structural performance and severe failures of materials and components (Ellingwood, 2005). The damage process induced by the diffusive attack from aggressive agents, such as chlorides, includes corrosion of reinforcement and deterioration of concrete (CEB, 1992; Kilareski, 1980). A proper modelling of these effects is essential to a life-cycle structural assessment. In recent years, relevant advances have been accomplished in the fields of life-cycle analysis and design of deteriorating civil engineering systems and novel approaches to time-variant assessment and optimisation of concrete structures in aggressive environment have been proposed (Biondini & Frangopol, 2008; Chen, Frangopol, & Ang, 2010; Cho, Frangopol, & Ang, 2007; Frangopol, 2011; Frangopol & Furuta, 2001; Furuta, Frangopol, & Akiyama, 2014; Frangopol, Kallen, & van Noortwijk, 2004; Nowak & Frangopol, 2005; Strauss, Frangopol, & Bergmeister, 2012).

The present paper deals with the assessment of soundness and accuracy of diffusion models used to study corrosion phenomena and related effects induced in reinforced concrete (RC) structures by the ingress of chlorides and other aggressive agents. Actually, chloride ions can penetrate by pure diffusion only in concrete that is completely saturated with water (Papakonstantinou & Shinozuka, 2013). In general, chloride ingress is a complex process which may involve several other mechanisms such as water surface absorption in partially saturated concrete, water flow in the outer part of the concrete volume where moisture conditions fluctuate quite significantly due to cycles of wetting and drying, and binding of chlorides with the cement past hydration products, among others (Bastidas-Arteaga, Chateauneuf, Sánchez-Silva, Bressolette, & Schoefs, 2011; Medeiros, Gobbi, Réus, & Helene, 2013; Yuan, Shi, De Schutter, Audenaert, & Deng, 2009). In addition, chloride diffusion and moisture transport are coupled mechanisms (Johannesson, 2003). Multi-mechanistic-coupled transport models of heat, moisture and various chemical substances are available in literature (Boddy, Bentz, Thomas, & Hooton, 1999; Saetta, Schrefler, & Vitaliani, 1993; Xi & Bažant, 1999; Xi, Willam, & Frangopol, 2000). However, they are computationally expensive and need detailed knowledge of site-specific environmental factors and a wide range of material properties that are rarely available for a proper model calibration (Papakonstantinou & Shinozuka, 2013; Vořechovská, Podroužek, Chromá, Rovnaníková, & Teplý, 2009). Fick's diffusion model is hence used as a convenient tool for predicting the onset of corrosion in practical applications, since observations indicate that the transport of chlorides in concrete is mainly diffusion controlled with a relatively small convection zone (Hunkeler, 2005). In this approach, the influence of various transport mechanisms on chloride penetration can be quantified by means of a modified time-variant diffusion coefficient in the concrete, generally referred to as the apparent diffusion coefficient (Duprat, 2007; fib, 2006; Nielsen & Geiker, 2003; Yuan et al., 2009). Sorption/reaction effects, including the influence of binding and its kinetics, can be incorporated in Fick's model by adding reaction terms to the standard diffusion equation (Bentz, Garboczi, Lu, Martys, Sakulich, & Weiss, 2013).

CONTACT Andrea Titi andrea.titi@polimi.it

In durability analysis and life-cycle assessment of concrete structures exposed to corrosion, Fick's diffusion model is frequently applied in a simplified one-dimensional (1D) form (fib, 2006). However, in most applications of practical interest the diffusion process is more properly described by two- or three-dimensional patterns of concentration gradients (Titi & Biondini, 2012). In this paper, the accuracy of the 1D modelling of diffusion and its impact on the life-cycle assessment of concrete structures under corrosion is evaluated in deterministic and probabilistic terms with respect to more accurate two-dimensional (2D) formulations. Since the focus is on the compliance of 1D vs. 2D diffusion models rather than on the capability of generalised models to reproduce complex transport processes, pure chloride diffusion with constant diffusivity is considered for the purpose of the comparison.

In the proposed study, the numerical solution of the diffusion problem is obtained by using a special class of evolutionary algorithm known as cellular automata. This approach has been proposed in previous works and applied to life-cycle reliability-based design, assessment and maintenance of concrete structures in aggressive environment (Biondini, Bontempi, Frangopol, & Malerba, 2004, 2006; Biondini, Camnasio, & Palermo, 2014; Biondini & Frangopol, 2009; Biondini, Frangopol, & Malerba, 2008). The proposed formulation is validated considering diffusion problems for which analytical closed-form solutions are known. Therefore, parametric analyses are carried out on solid and hollow-core rectangular cross-sections with different aspect ratios and exposures to compare the results of 1D and 2D modelling. The effects of the uncertainty involved in the problem are also considered by comparing the probability density distributions of the corrosion initiation time. The influence of the diffusion modelling on the time-variant corrosion damage of RC cross-sections is finally studied in deterministic and probabilistic terms with reference to the local damage of the reinforcing steel bars and the global deterioration of the bending moment vs. curvature capacity curves. The results show that 1D diffusion models can lead to a significant loss of accuracy over time depending on the aspect ratio of the cross-section, location of the reinforcing steel bars and exposure conditions. Consequently, 2D diffusion simulations may be necessary and are generally recommended for accurate life-cycle assessment of concrete structures exposed to corrosion.

Cellular automata simulation of diffusion processes

Modelling of diffusion processes

The diffusion of chemical components in solids can be described by relating the rate of mass diffusion to the concentration gradients responsible for the net mass transfer. The simplest model is represented by Fick's first law, which assumes a linear relationship between the mass flow and the concentration gradient. The combination of Fick's model with the mass conservation principle leads to Fick's second law which, in the case of single component diffusion in isotropic, homogeneous and time-invariant media, can be reduced to the following second-order partial differential linear equation (Glicksman, 2000):

$$D\nabla^2 C = \frac{\partial C}{\partial t} \tag{1}$$

where D is the diffusivity coefficient of the medium, $C = C(\mathbf{x}, t)$ is the concentration of the chemical component at point $\mathbf{x}=(x, y, z)$ and time t, $\nabla C = \mathbf{grad}\ C(\mathbf{x}, t)$ and $\nabla^2=\nabla\cdot\nabla$.

Closed-form analytical solutions of Fick's differential equation are available only for simple problems. In general, numerical procedures are necessary to deal with arbitrary spatial domains and complex boundary conditions. Several numerical methods can be used to solve the diffusion equation (Quarteroni, Sacco, & Saleri, 2007). In this study, the numerical solution is achieved using cellular automata (Biondini et al., 2004).

Cellular automata

Cellular automata were firstly introduced and pioneered by von Neumann and Ulam in the early 50s (von Neumann, 1966) and subsequently developed by other researchers in many fields of science (Margolus & Toffoli, 1987; Schiff, 2008; Wolfram, 1994, 2002). Basically, they represent simple mathematical idealisations of physical systems in which space and time are discrete, and physical quantities can assume only a finite set of discrete values. In fact, any physical system satisfying differential equations may be approximated as a cellular automaton by introducing discrete coordinates and variables, as well as discrete time steps.

In its basic form, a cellular automaton consists of a regular uniform grid of sites or cells, theoretically having infinite extension, with a state variable associated with each cell. The state of the cellular automaton at time t is then completely specified by the values $s_i = s_i(t)$ of the variables at each cell i. Cellular automata evolve in discrete time steps according to a parallel state transition determined by a set of local rules: the variables $s_i^{k+1} = s_i(t_{k+1})$ at each site i at time t_{k+1} are updated synchronously based on the values of the variables s_n^k in their 'neighbourhood' n at the preceding time instant t_k. The neighbourhood n of a cell i usually consists of the cell itself and a set of adjacent cells within a given radius r, or $(i - r) \le n \le (i + r)$. Figure 1 presents an example of typical neighbourhoods for 2D cellular automata with $r = 1$, but patterns of higher complexity can be also proposed.

In general, any physical system satisfying differential equations may be approximated as a cellular automaton by introducing discrete coordinates and state variables, as well as discrete time steps. Properly, therefore, models based on cellular automata provide an alternative and more general approach to physical modelling rather than an approximation. They exhibit a complex behaviour analogous to that associated with complex differential equations, but in this case complexity emerges from the interaction of simple entities following simple rules. Noteworthy examples of cellular automata modelling of physical processes

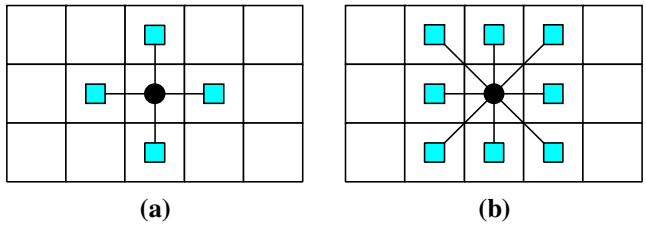

Figure 1. Neighbourhoods for 2D cellular automata with radius $r = 1$: (a) von Neumann; (b) Moore.

in concrete have been proposed, including models for microstructure development of cement hydration (Bentz, Coveney, Garboczi, Kleyn, & Stutzman, 1994) and damage processes under corrosion (Biondini et al., 2004) and fire (Biondini & Nero, 2011).

Solution of the diffusion equation

Cellular automata represent an effective tool for the numerical solution of partial differential equations which describe diffusion processes or multi-physics problems (Vick, 2007). In particular, the diffusion process described by Fick's laws in d dimensions ($d = 1, 2, 3$) can be effectively simulated by adopting a von Neumann neighbourhood with radius $r = 1$ (Figure 1(a)) and the following evolutionary rule (Biondini et al., 2004):

$$C_i^{k+1} = \phi_0 C_i^k + \sum_{j=1}^{d} (\phi_j^- C_{i-1,j}^k + \phi_j^+ C_{i+1,j}^k) \tag{2}$$

where the state variable $s_i^k = C_i^k = C(\mathbf{x}_i, t_k)$ represents the concentration in the cell i at time t_k, and ϕ_0, ϕ_j^- and $\phi_j^+ (j = 1, \dots, d)$ are evolutionary coefficients. A proof can be found in related studies (Biondini, 2011; Biondini et al., 2008).

According to the mass conservation law, the evolutionary coefficients must satisfy the following normality rule:

$$\phi_0 + \sum_{j=1}^{d} (\phi_j^- + \phi_j^+) = 1 \tag{3}$$

For isotropic media, in order to avoid directionality effects, the symmetry condition $\phi_j^- = \phi_j^+ = \phi_1 (j = 1, \dots, d)$ must be adopted, with $\phi_0 = (1 - 2d\phi_1)$. Therefore, in case of mass diffusion in an isotropic medium, the following evolutionary rule holds:

$$C_i^{k+1} = \phi_0 C_i^k + \frac{1 - \phi_0}{2d} \sum_{j=1}^{d} (C_{i-1,j}^k + C_{i+1,j}^k) \tag{4}$$

The grid dimension Δx and time step Δt of the cellular automaton should be chosen consistently with the required level of accuracy. In addition, once a value of the central evolutionary coefficient ϕ_0 is chosen, the diffusion process can be regulated according to a given value of the diffusion coefficient D by relating the grid dimension Δx and time step Δt as follows (Biondini et al., 2004):

$$\frac{\Delta x^2}{\Delta t} = \frac{2d}{1 - \phi_0} D \tag{5}$$

A suitable value of the central evolutionary coefficient in case of constant diffusivity is $\phi_0 = 1/2$. As previously mentioned, pure chloride diffusion with constant diffusivity is considered in this study. However, in concrete structures diffusivity can change over time and cracking may induce local modifications in the rate of mass diffusion which usually involve higher gradient of concentration and coupling effects between diffusion and damage (Bentz et al., 2013; Biondini et al., 2004; Garces Rodriguez & Hooton, 2003; Papakonstantinou & Shinozuka, 2013). The variation in space and time of the diffusion coefficient can be taken into account in the cellular automata solution of the diffusion equation by considering the evolutionary coefficients as time-variant with higher values in cracked regions depending on the crack width. The stochastic effects in the mass transfer associated with the local random variability of the material diffusivity can also be considered by assuming the evolutionary coefficients as random variables. Additional information and modelling guidelines can be found in Biondini et al. (2004).

Validation of the cellular automata formulation

The numerical validation of the proposed cellular automata formulation of the diffusion equation is reported elsewhere (Biondini, 2011). In the following, the high accuracy of this formulation is shown for 1D and 2D diffusive problems with closed-form analytical solution.

1D medium with localised source

The solution of the 1D diffusion in a semi-infinite medium $x \geq 0$ with a source of constant concentration C_0 localised at $x = 0$ is described by the following function:

$$C(x, t) = C_0 \left[1 - \mathrm{erf}\left(\frac{x}{2\sqrt{Dt}} \right) \right] \tag{6}$$

where erf(•) is the Gauss error function. In this equation, the quantity $\lambda = 2\sqrt{Dt}$ is called the diffusion length and provides a measure of how far the concentration has propagated in the x-direction by diffusion in time t (Bird, Stewart, & Lightfoot, 2002). Figure 2 shows the concentration profiles at time $t = 10$ years and $t = 50$ years associated with a chloride concentration $C_0 = 3.0$ wt.-%/c and a diffusion coefficient $D = 10^{-11}$ m^2/s, which corresponds to cement class CEM I 42.5 R with water to cement ratio $w/c = 0.45$ (fib, 2006). The analytical solution is compared with the numerical solution obtained by means of a cellular automaton with $\phi_0 = 1/2$ and $\Delta x = 0.01$ m. The comparison shows the very good accuracy of the numerical solution.

2D medium with insulating boundaries

A 2D medium with spatial domain $0 \leq x \leq L$ and $0 \leq y \leq H$ is considered. The medium is insulated along the sides in the x-direction ($y = 0$ and $y = H$) and the concentration is kept to zero along the sides in the y-direction ($x = 0$ and $x = L$), as shown in

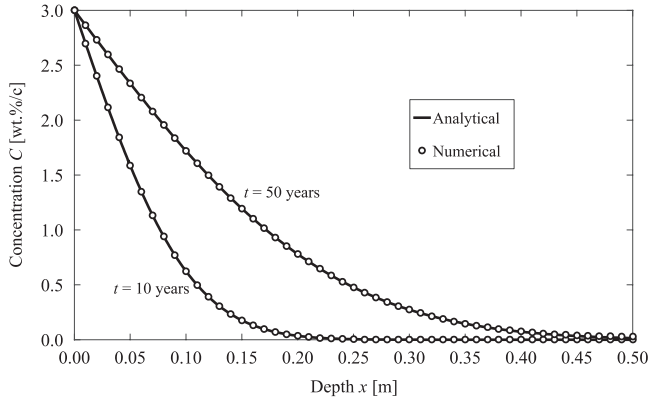

Figure 2. Concentration profiles $C = C(x, t)$ for a 1D diffusion with localised source: comparison between analytical and numerical results.

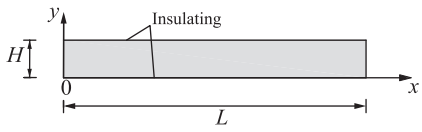

Figure 3. 2D medium with insulating boundaries.

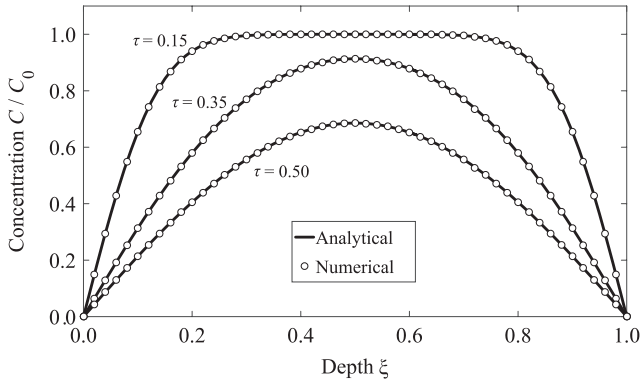

Figure 4. Concentration profiles for a 2D medium with insulating boundaries: comparison between analytical and numerical results at time instants $\tau = 0.15$, 0.35 and 0.50.

Figure 3. At the initial time, a uniform constant concentration C_0 is assumed over the spatial domain. Therefore, the boundary conditions are as follows:

$$\begin{cases} C(x, y, t = 0) = C_0 \\ C(x = 0, y, t) = C(x = L, y, t) = 0 \end{cases} \tag{7}$$

The analytical solution of the problem depends on the x-coordinate only and it can be expressed in terms of a Fourier series as follows (Crank, 1975):

$$C(x, y, t) = C(x, t) = \frac{4C_0}{\pi} \sum_{n=0}^{\infty} \frac{1}{2n+1} \mathrm{e}^{-\left[\frac{(2n+1)\pi}{L}\right]^2 Dt} \sin \frac{(2n+1)\pi x}{L} \tag{8}$$

Figure 4 shows the profiles of concentration $C(x, t)/C_0$ vs. the normalised coordinate $\xi = x/L$ at the time instants associated with a normalised diffusion length $\tau = \lambda/L = 0.15$, 0.35, and 0.50, where λ is the diffusion length for 1D diffusion. The analytical solution is compared with the numerical solution obtained for $H = L/8$ by means of a cellular automaton with $\phi_0 = 1/2$ and $\Delta x = L/400$. This comparison confirms the very good accuracy of the numerical model.

2D medium with sinusoidal initial concentration

A 2D medium with spatial domain $0 \le x \le L$ and $0 \le y \le H$ is considered. The following sinusoidal-type distribution of concentration is assumed at the initial time:

$$C(x, y, t = 0) = C_0 \sin \frac{2n\pi x}{L} \sin \frac{2m\pi y}{H} \tag{9}$$

where C_0 is the initial concentration value at sinusoidal peaks. The analytical solution of the diffusion equation is as follows:

$$C(x, y, t) = C_0 \mathrm{e}^{-\left[\left(\frac{2n\pi}{L}\right)^2 + \left(\frac{2\pi m}{H}\right)^2\right] Dt} \sin \frac{2n\pi x}{L} \sin \frac{2m\pi y}{H} \tag{10}$$

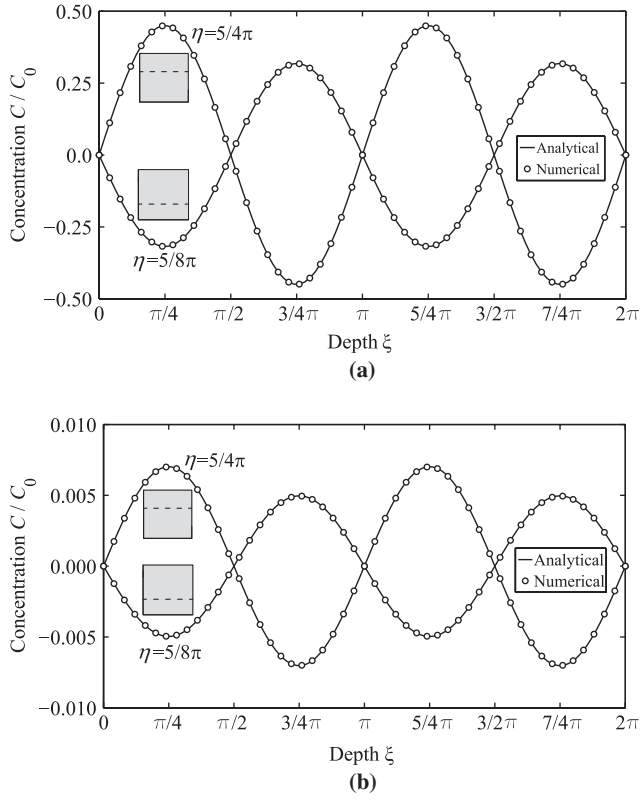

Figure 5. Concentration profiles for a 2D medium with sinusoidal initial concentration: comparison between analytical and numerical results at time instants (a) $\tau = 0.10$ and (b) $\tau = 0.25$.

A case study with $n = m = 2$ and $H = L$ is presented (Karaa & Zhang, 2004). Figure 5 shows the profiles of concentration $C(x, y, t)/C_0$ vs. the normalised coordinate $\xi = 2\pi x/L$ for different values of the normalised coordinate $\eta = 2\pi y/L$ ($\eta = 5/8\pi$ and $\eta = 5/4\pi$) and different time instants referred to a normalised diffusion length $\tau = \lambda/L$, namely, $\tau = 0.10$ (Figure 5(a)) and $\tau = 0.25$ (Figure 5(b)). The analytical solution is compared with the numerical solution obtained by means of a cellular automaton with $\phi_0 = 1/2$ and $\Delta x = L/200$. This comparison shows once again the very good accuracy of the numerical model.

Accuracy of 1D diffusion models

The closed-form solution of the Fickian 1D diffusion with localised source, given by Equation (6), is frequently used in practical application to assess the chloride profiles and corrosion initiation time in concrete structures (Biondini et al., 2014; Enright & Frangopol, 1998; Estes & Frangopol, 1999; Frangopol, Lin, & Estes, 1997; Glass & Buenfeld, 2000; Vu & Stewart, 2000). In the following, the accuracy of this approach is investigated by comparing the 1D closed-form solution with the results provided by more general 2D diffusion models applied to solid and hollow-core cross-sections.

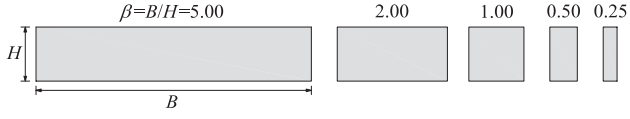

Figure 6. Rectangular solid cross-sections with different aspect ratio $\beta = B/H$.

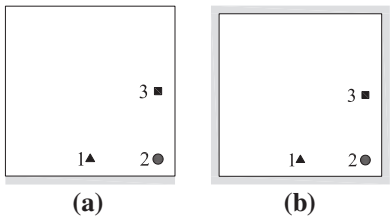

Figure 7. Exposure scenarios and location of the monitoring points: diffusion from (a) one side and (b) four sides.

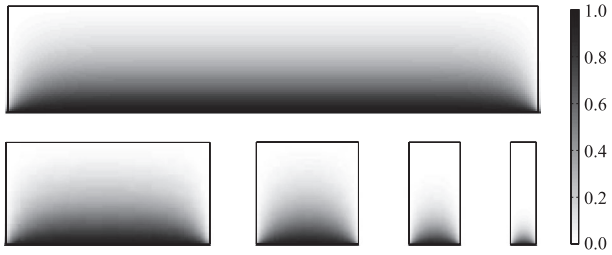

Figure 8. Maps of 2D concentration $C(x, y)/C_0$ evaluated at the time instant $\tau = 0.50$ for the rectangular cross-sections shown in Figure 6 with exposure on one side (Figure 7(a)).

Solid cross-sections

Solid rectangular cross-sections with varying aspect ratio $\beta = B/H$, as shown in Figure 6, are considered. The two exposure scenarios described in Figure 7, with a localised source of constant concentration C_0 located along one side (Figure 7(a)) and four sides (Figure 7(b)), are investigated.

The 1D diffusion front is uniform along the entire cross-section width. However, the 2D diffusion front is non-uniform. This is clearly illustrated in Figure 8, which shows the concentration contour maps evaluated at the time instant associated with a normalised diffusion length $\tau = \lambda/H = 0.50$ for the cross-sections shown in Figure 6 exposed to diffusion from one side. A good agreement between 1D and 2D modelling can be achieved for high values of the aspect ratio $\beta = B/H$, with convergent results for $\beta \to \infty$. In fact, if $B >> H$, the 2D concentration profiles tend to be uniform since the effect of boundaries is limited to a region close to the external sides. On the contrary, if $B << H$, the influence of the boundaries is reflected along the entire cross-section width, and the approximation provided by the 1D uniform concentration front is not accurate.

Table 1. Threshold value $\hat{\beta}$ of the aspect ratio associated with a target error $\hat{e}$ at point 1 with edge distance ξ under diffusion from one side (Figure 7(a)).

Target error $\hat{e}$ [%]	$\xi = 0.05$	$\xi = 0.10$
1	1.89	2.43
2	1.47	1.92
5	0.98	1.40
10	0.67	0.99

The error associated with the difference between 1D and 2D diffusion processes is evaluated as follows:

$$e = \frac{C^{1D} - C^{2D}}{C^{1D}} \tag{11}$$

where C^{1D} and C^{2D} are the concentration functions obtained from the solution of the 1D and 2D diffusion equations, respectively. The error is computed for cross-sections with aspect ratio varying between 0.2 and 5.0 at three points located near the cross-section edges, as shown in Figure 7, for different values of the normalised edge distance $\xi = x/H$. Figure 9 compares the errors for diffusion from one side at the monitoring points 1, 2 and 3, for $\xi = 0.05$ (Figure 9(a)) and $\xi = 0.10$ (Figure 9(b)) at the normalised time instant $\tau = 1.00$. These results indicate that a good agreement between 1D and 2D modelling is achieved at point 1 for $\beta > 1$. The threshold values $\hat{\beta}$ associated with target error values $\hat{e} = 1$, 2, 5 and 10% are listed in Table 1. Contrary, at point 1 for $\beta < 1$ and at points 2 and 3 for all β-values, the 1D solution significantly overestimates the actual 2D concentration. In case of exposure on four sides, the errors at points 1, 2 and 3 are compared in Figure 10. These results indicate that the 1D solution leads in all cases to underestimate the actual 2D concentration with errors $e > 4\%$.

The largest scatter between 1D and 2D diffusion occurs at point 2, since in the corner region the 1D modelling cannot capture the local effects of combined diffusion from the two adjacent sides. In practical applications, these effects are often approximated by superposing the effects of 1D diffusion from the exposed sides of the cross-section:

$$C(x, y) = \sum_{k=1}^{4} C_k^{1D}(x, y) \tag{12}$$

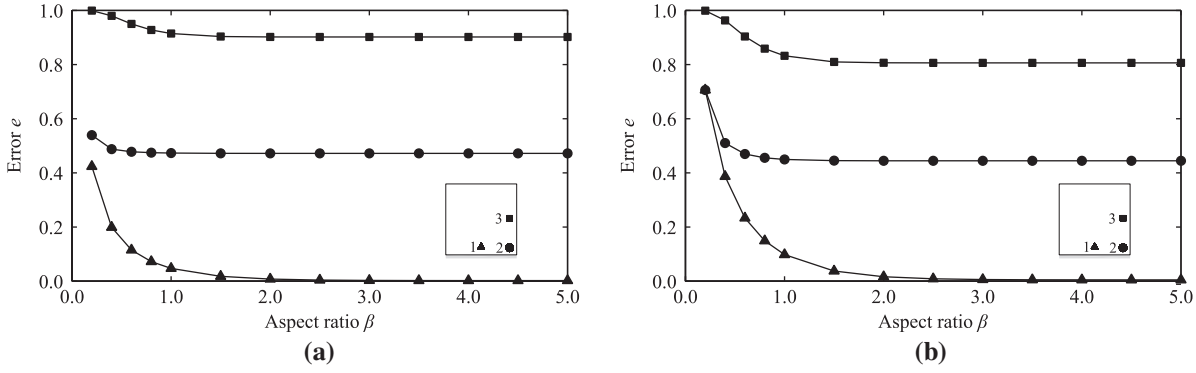

Figure 9. Exposure scenario with diffusion from one side: error estimate of the 1D diffusion modelling computed at time instant $\tau = 1.00$ at the monitoring points 1, 2, and 3 with edge distance (a) $\xi = 0.05$ and (b) $\xi = 0.10$.

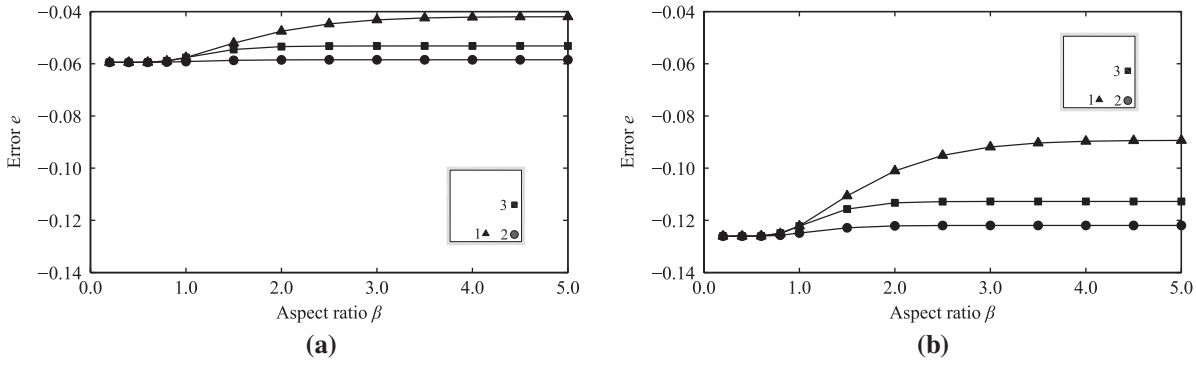

Figure 10. Exposure scenario with diffusion from four sides: error estimate of the 1D diffusion modelling computed at time instant $\tau = 1.00$ at the monitoring points 1, 2 and 3 with edge distance (a) $\xi = 0.05$ and (b) $\xi = 0.10$.

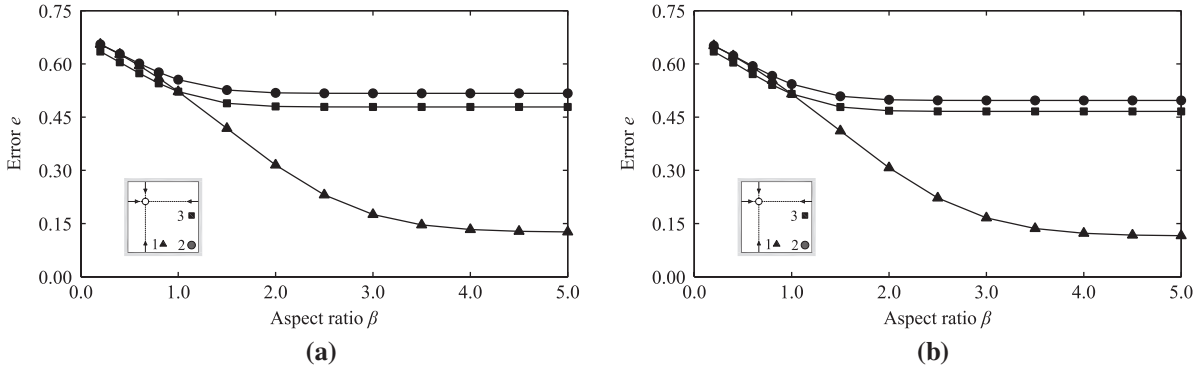

Figure 11. Exposure scenario with diffusion from four sides: error estimate of the superposition of 1D diffusion from four sides computed at time instant $\tau = 1.00$ at the monitoring points 1, 2 and 3 with edge distance (a) $\xi = 0.05$ and (b) $\xi = 0.10$.

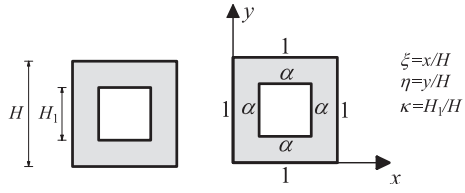

Figure 12. Hollow-core square cross-section: geometrical parameters and exposure scenario.

where $C_k^{1D} = C_k^{1D}(x, y)$ is the concentration analytical function associated with the 1D diffusion from side k, with $k = 1,2,3,4$. However, as shown in Figure 11, this approach may also lead to very inaccurate results, with an overestimation of the actual 2D concentration.

Hollow-core cross-sections

The hollow-core square cross-section presented in Figure 12 is considered. The cross-section is exposed along the external and internal surfaces with concentration C_0 and αC_0, respectively, with $0 \le \alpha \le 1$. This case is of practical interest since structural members with hollow cross-section, such as bridge piers, may be not hermetically closed over the volume with their internal surface exposed to atmospheric conditions (Biondini et al., 2014). The 2D diffusion problem is solved numerically for different values of the normalised core size $\kappa = H_1/H$ and two exposure scenarios with $\alpha = 0$ and $\alpha = 1$. The solutions of the 1D and 2D diffusion problems are compared in Figures 13–16, which show the concentration $C(x, y, t)/C_0$ vs. the normalised time $\tau = \lambda/H$ at selected monitoring points with normalised coordinates $\xi = x/H$ and $\eta = y/H$.

These results confirm that the 1D solution significantly underestimates the actual level of concentration at points located in the corner regions (Figures 13 and 14), where the 1D modelling is unable to reproduce the local effects of combined diffusion from the two adjacent sides. The accuracy of the 1D solution is generally low also at points located far from the corner regions (Figures 15 and 16), where the concentration tends to be significantly overestimated with external exposure ($\alpha = 0$) and underestimated with full exposure ($\alpha = 1$). At these points, the 1D analytical solution provides a good accuracy only for small core size ratio and at the early stage of the diffusion process.

Influence of diffusion modelling on life-cycle assessment

The objective of a life-cycle structural analysis is to evaluate the effects of diffusion in terms of corrosion damage and evolution over time of the structural performance. To this purpose, the influence of the diffusion modelling on the time-variant corrosion damage of RC cross-sections is studied in deterministic and probabilistic terms with reference to the local damage of the reinforcing steel bars and the global deterioration of the bending

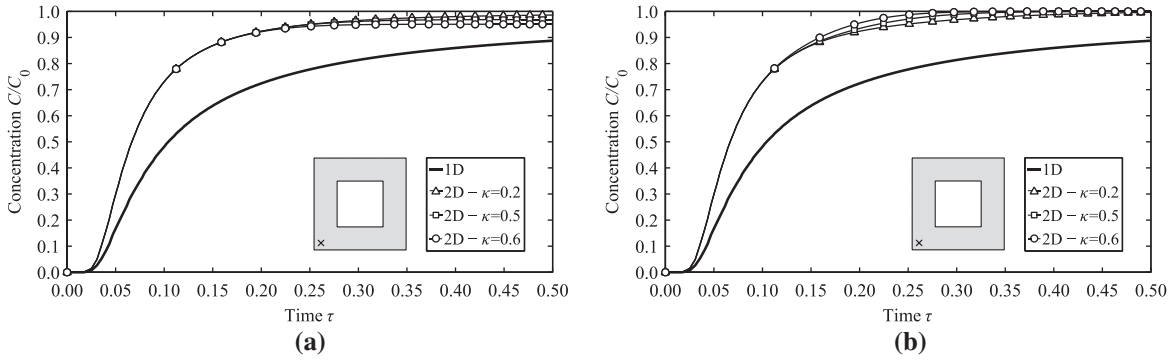

Figure 13. Comparison between 1D and 2D diffusion in terms of time history of concentration at coordinates $\xi = \eta = 0.05$ for different core width ratio k with exposure (a) $\alpha = 0$ and (b) $\alpha = 1$.

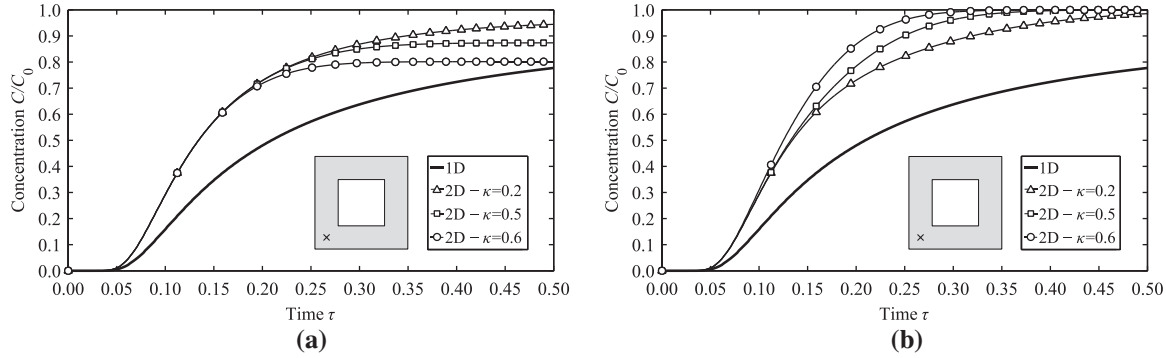

Figure 14. Comparison between 1D and 2D diffusion in terms of time history of concentration at coordinates $\xi = \eta = 0.10$ for different core width ratio k with exposure (a) $\alpha = 0$ and (b) $\alpha = 1$.

moment vs. curvature capacity curves. Since the focus is on the compliance of 1D vs. 2D diffusion models, pure chloride diffusion with constant diffusivity and no chloride binding is considered for the purpose of the comparison. It is worth noting that these assumptions are conservative for practical applications, since diffusivity tends to decrease over time (fib, 2006; Tang & Gulikers, 2007) and binding of the chloride ions by the cement paste reduces the rate of chloride ingress (Bentz et al., 2013; Yuan et al., 2009).

Corrosion initiation and propagation

The main effect of corrosion in concrete structures is the mass loss of the reinforcing steel bars. The percentage loss of steel resistant area of a corroded bar can be described by means of a dimensionless damage index $\delta_s = \delta_s(t)$ which provides a direct measure of deterioration within the range [0,1]. The area A_s of the corroded bar can be represented as a function of the damage index as follows (Biondini et al., 2004):

$$A_s(t) = \left[1 - \delta_s(t)\right] A_{s0} \tag{13}$$

where A_{s0} is the area of the undamaged bar.

The corrosion process may also involve a remarkable reduction of steel ductility even for a limited amount of mass loss (Almusallam, 2001; Apostolopoulos & Papadakis, 2008). Moreover, the formation of oxidation products may lead to the development of longitudinal splitting cracks in the concrete surrounding the corroded bars and, consequently, to delaminating and spalling of the concrete cover (Al-Harthy, Stewart, & Mullard, 2011; Cabrera, 1996; Guzmán, Gálvez, & Sancho, 2011; Vidal, Castel, & François, 2004; Zhang, Castel, & François, 2010). Based on experimental evidence, these damage effects depend on the amount of mass loss and can be effectively modelled by relating the ultimate steel strain ε_{su} of the corroded bars and the compression strength f_c of the surrounding concrete to the damage index δ_s. The formulation of the deteriorating functions $\varepsilon_{su} = \varepsilon_{su}(\delta_s)$ and $f_c = f_c(\delta_s)$, as well as the numerical validation against experimental results of the damage model adopted in this study, can be found in Biondini & Vergani (2015).

The evolution in time of corrosion damage is related to the corresponding evolution of the diffusive process. In fact, when deterioration is induced by aggressive agents, such as chlorides, the rate of damage depends, among other factors, on the level of concentration of the substance which diffuses inside the structure (Bertolini, 2008). Based on available data for corrosion rate under sulphate and chloride attacks (Bertolini, Elsener, Pedeferri, & Polder, 2004; Pastore & Pedeferri, 1994), the damage rate at time t of a reinforcing steel bar located at point $\mathbf{x}$ is evaluated as follows (Biondini et al., 2004):

$$\frac{\partial \delta_s(t)}{\partial t} = q_s C(\mathbf{x}, t), \quad t \geq t_i \tag{14}$$

where $q_s = (C_s \Delta t_s)^{-1}$ is a damage rate coefficient, C_s is the value of constant concentration leading to complete damage of the steel bar after the time interval Δt_s, and t_i is the corrosion initiation

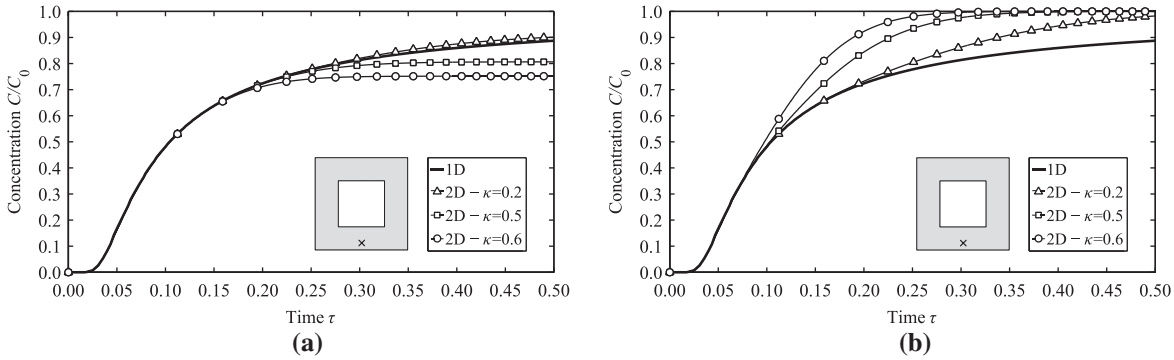

Figure 15. Comparison between 1D and 2D diffusion in terms of time history of concentration at coordinates $\xi = 0.50$ and $\eta = 0.05$ for different core width ratio k with exposure (a) $\alpha = 0$ and (b) $\alpha = 1$.

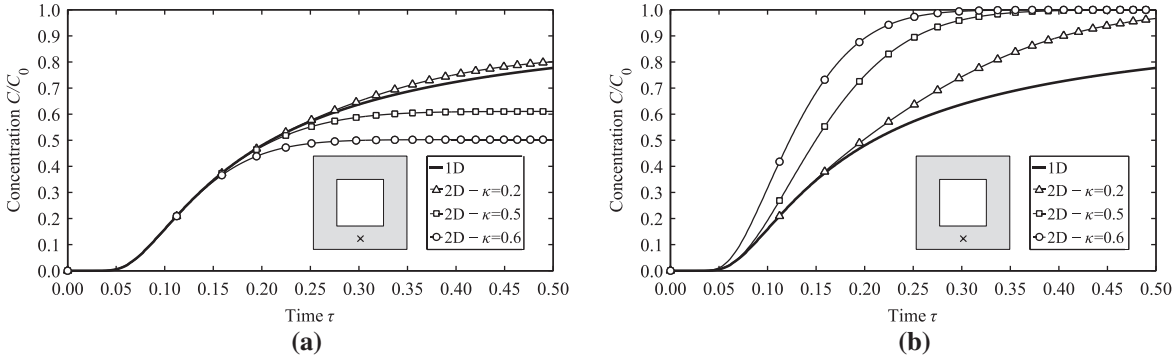

Figure 16. Comparison between 1D and 2D diffusion in terms of time history of concentration at coordinates $\xi = 0.50$ and $\eta = 0.10$ for different core width ratio k with exposure (a) $\alpha = 0$ and (b) $\alpha = 1$.

time. The coefficient q_s depends on the rate of corrosion penetration and type of corrosion mechanism, i.e. generalised (uniform) or localised (pitting) corrosion (Biondini & Vergani, 2015). The initiation time t_i is associated with the attainment of a critical threshold of concentration C_{cr}, or $t_i = \min\{ t \mid C(\mathbf{x}, t) \geq C_{cr}\}$. The analytical solution of the 1D diffusion equation is frequently used to assess the corrosion initiation time as follows:

$$t_i = \frac{c^2}{4D}\left[\text{erf}^{-1}\left(\frac{C_0 - C_{cr}}{C_0}\right)\right]^{-2} \tag{15}$$

where c is the concrete cover. However, for 2D diffusion processes with arbitrary boundary conditions the corrosion initiation time has to be computed numerically.

Time-variant structural performance of RC cross-sections

The time-variant structural performance of the solid and hollow-core square RC cross-sections shown in Figure 17 is investigated. The nominal values of material strengths and strain limits are, respectively, $f_c = 38$ MPa and $\varepsilon_{cu} = 0.35\%$ for concrete in compression, and $f_{sy} = 450$ MPa and $\varepsilon_{su} = 7.5\%$ for reinforcing steel. The effects of the confinement action of the stirrups are taken into account based on the model proposed by Mander, Priestley, and Park (1988). Chloride ingress is studied in the nominal case by assuming a diffusivity coefficient $D = 1.58 \times 10^{-11}$ m^2/s and the exposure scenarios shown in Figures 7 and 12, with chloride concentration $C_0 = 3.0$ wt.-%/c at the exposed external surfaces and a critical threshold of concentration $C_{cr} = 0.6$ wt.-%/c (fib, 2006). The corrosion damage induced by diffusion is evaluated by assuming a steel damage rate coefficient $q_s = (C_s \Delta t_s)^{-1}$ with $C_s = C_0$ and $\Delta t_s = 50$ years. These case studies reproduce deterioration processes with severe damage of the materials, as it may occur for heavily chloride-contaminated concrete and high relative humidity (Bertolini et al., 2004).

Life-cycle structural analyses are carried out over a 50-year lifetime and the results provided by 1D and 2D diffusion models are compared. Figure 18 shows the evolution over time of the damage index δ_s of the steel bars #1 and #2 of the solid RC cross-section under diffusion from one side (Figure 18(a)) and four sides (Figure 18(b)). The steel bars #1 and #2 have a different exposure to chloride attack and are expected to suffer over time a different amount of damage. This difference is well described by the 2D model, but it is not captured by the 1D model which leads to the same amount of damage for all the steel bars located at the same depth. The error associated with 1D diffusion is hence higher for the bars located in the corner regions and involves a significant overestimation of damage for the exposure scenario with diffusion from one side, and a significant underestimation with diffusion from four sides.

Similar results are obtained for the hollow-core RC cross-section, as shown in Figure 19 for the damage index δ_s of the steel bars #1 and #2 under external exposure only (Figure 19(a)) and full exposure of both external and internal surfaces (Figure 19(b)). It is noted that the 1D model leads to underestimate the damage of the steel bar #1 located in the

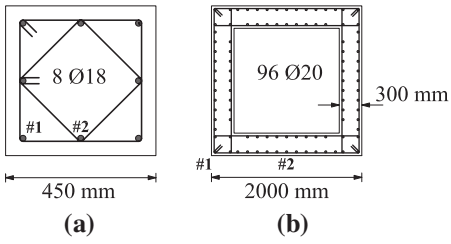

Figure 17. Geometry and reinforcement layout of square RC cross-sections: (a) solid cross-section; (b) hollow-core cross-section.

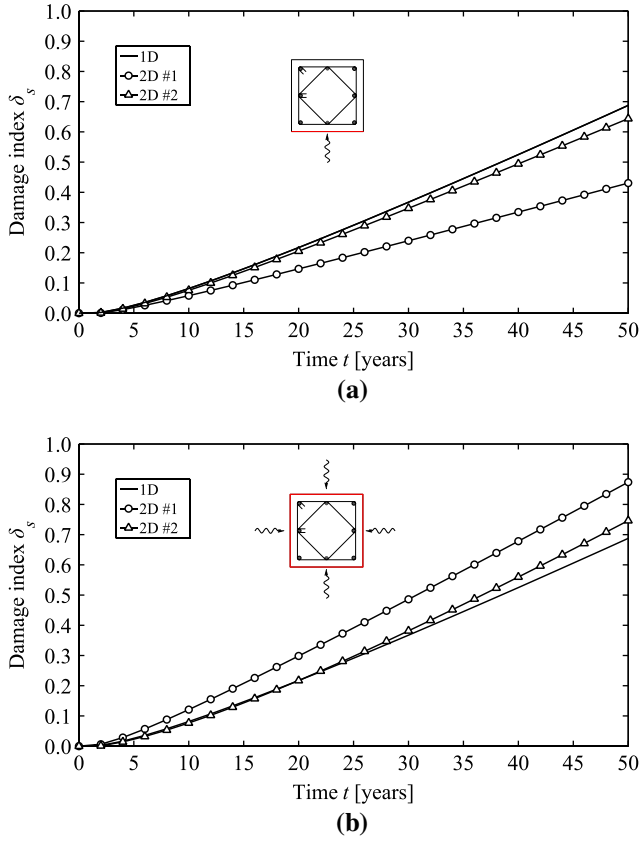

Figure 18. Evolution over time of the damage index δ_s of the steel bars #1 and #2 of the solid RC cross-section (Figure 17(a)) under diffusion from (a) one side ($\alpha = 0$) and (b) four sides ($\alpha = 1$).

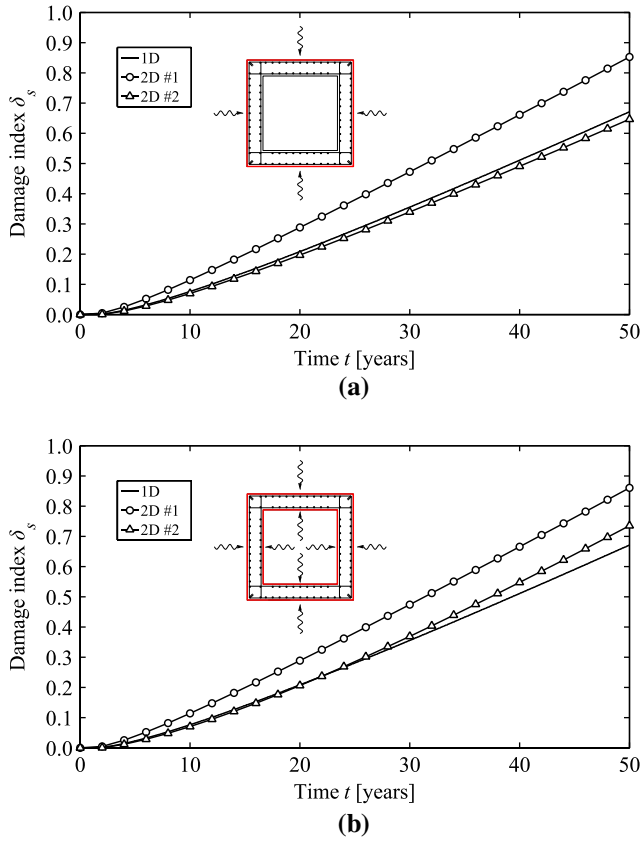

Figure 19. Evolution over time of the damage index δ_s of the steel bars #1 and #2 of the hollow-core RC cross-section (Figure 17(b)) under (a) external exposure only ($\alpha = 0$) and (b) full exposure of both external and internal surfaces ($\alpha = 1$).

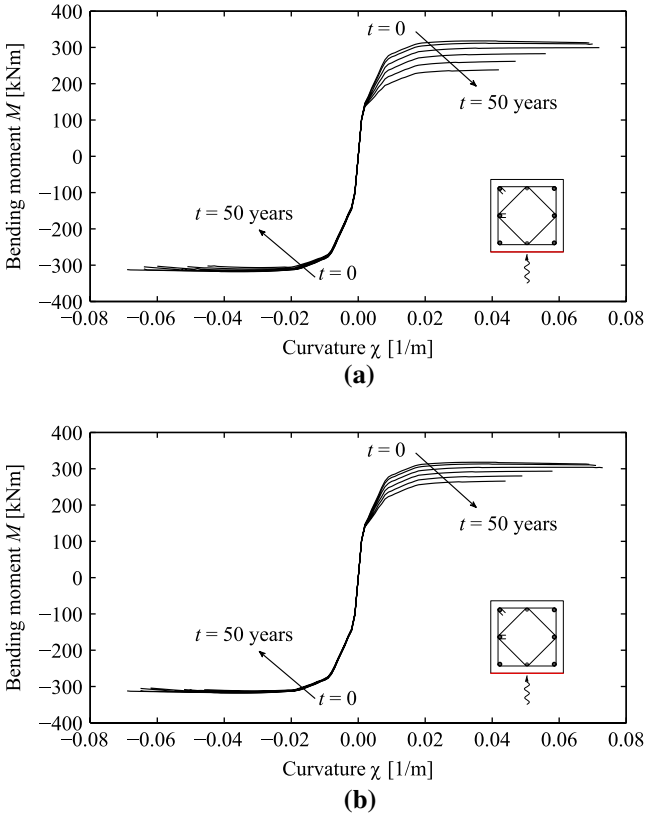

Figure 20. Evolution over time of the bending moment–curvature capacity curves of the solid RC cross-section exposed on one side ($\alpha = 0$): (a) 1D diffusion; (b) 2D diffusion.

corner, with similar error for the two exposure scenarios. For the steel bar #2 the error of the 1D model is smaller, but with a different trend depending on the exposure scenario. In fact, steel damage is overestimated in case of external exposure only and underestimated in case of full exposure.

The effects of local corrosion damage on the lifetime structural performance of the RC cross-sections are evaluated in terms of time-variant bending moment M vs. curvature χ capacity under axial force N. For the sake of brevity, only the results achieved for the solid cross-section under N=0.8 MN are presented herein. Figures 20 and 21 show the capacity curves under diffusion from one side (Figure 20) and four sides (Figure 21). It is worth nothing that for diffusion from one side ($\alpha = 0$) the exposure condition is not symmetric and the bending strength significantly decreases

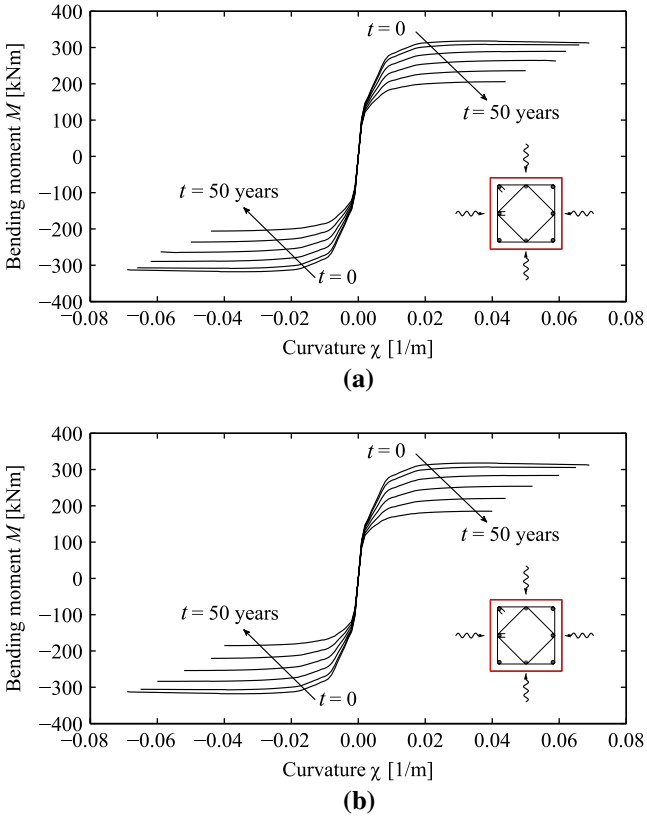

Figure 21. Evolution over time of the bending moment–curvature capacity curves of the solid RC cross-section exposed on four sides ($\alpha = 1$): (a) 1D diffusion; (b) 2D diffusion.

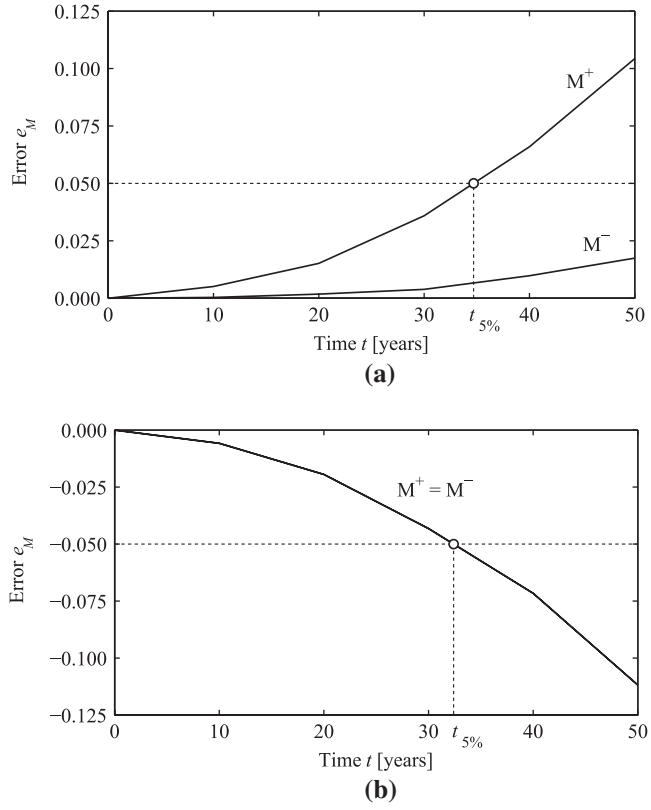

Figure 22. Time-variant error estimate of the 1D diffusion modelling in terms of bending strength capacity of the solid RC cross-section under diffusion from (a) one side ($\alpha = 0$), and (b) four sides ($\alpha = 1$).

only for $M > 0$, since the bars in tension are located in the most exposed part of the cross-section.

However, this is under condition that the stirrup spacing is sufficiently limited to avoid buckling of the compressive bars and consequent cover spalling, which may seriously affect the cross-sectional bending strength and curvature ductility also for $M < 0$. In any case, for the partial exposure scenario the comparison of the capacity curves in Figures 20(a) and (b) confirms that the 1D diffusion model leads over time to overestimate the effects of structural deterioration, with lower values of both bending strength capacity and curvature ductility. On the contrary, for the most severe exposure scenario with diffusion from four sides ($\alpha = 1$), the comparison of the capacity curves in Figures 21(a) and (b) indicates that the 1D diffusion model leads to underestimate the effects of structural deterioration on both bending strength capacity and curvature ductility.

The error of the 1D modelling in terms of bending strength capacity is quantified in Figure 22, which depicts the evolution over time of the following error function:

$$e_M = \frac{M^{2D} - M^{1D}}{M^{2D}} \tag{16}$$

where M^{1D} and M^{2D} are the time-variant resistant bending moments associated with 1D and 2D diffusion modelling, respectively. The error increases over time for both positive M^+ and negative M^- resistant bending moments, and reaches absolute values $|e_M| = 5\%$ after about 30–35 years of lifetime. However, it is worth noting that error values $e_M > 0$ are on the safe side. Contrary, error values $e_M < 0$ may be critical for structural safety.

Uncertainty modelling and probabilistic analysis

Due to uncertainties in material and geometrical properties and in the physical models of diffusion and damage processes, a probabilistic life-cycle measure of the time-variant structural performance is necessary for realistic results. For this reason, it

Table 2. Probability distributions and coefficients of variation (μ = mean value).

Random variable ($t = 0$)	Distribution type	C.o.V.
Concrete strength, f_c	Lognormal	5 MPa/μ
Steel strength, f_{sy}	Lognormal	30 MPa/μ
Diffusivity, D	Normal(*)	0.20
Damage rate, q_s	Normal(*)	0.30
Chloride concentration, C_0	Normal(*)	0.30
Critical concentration, C_{crit}	Beta(**)	0.25

(*)Truncated distributions with non-negative outcomes.
(**)Lower bound $b_{min} = 0.2$ wt.-%/c; Upper bound $b_{max} = 2.0$ wt.-%/c.

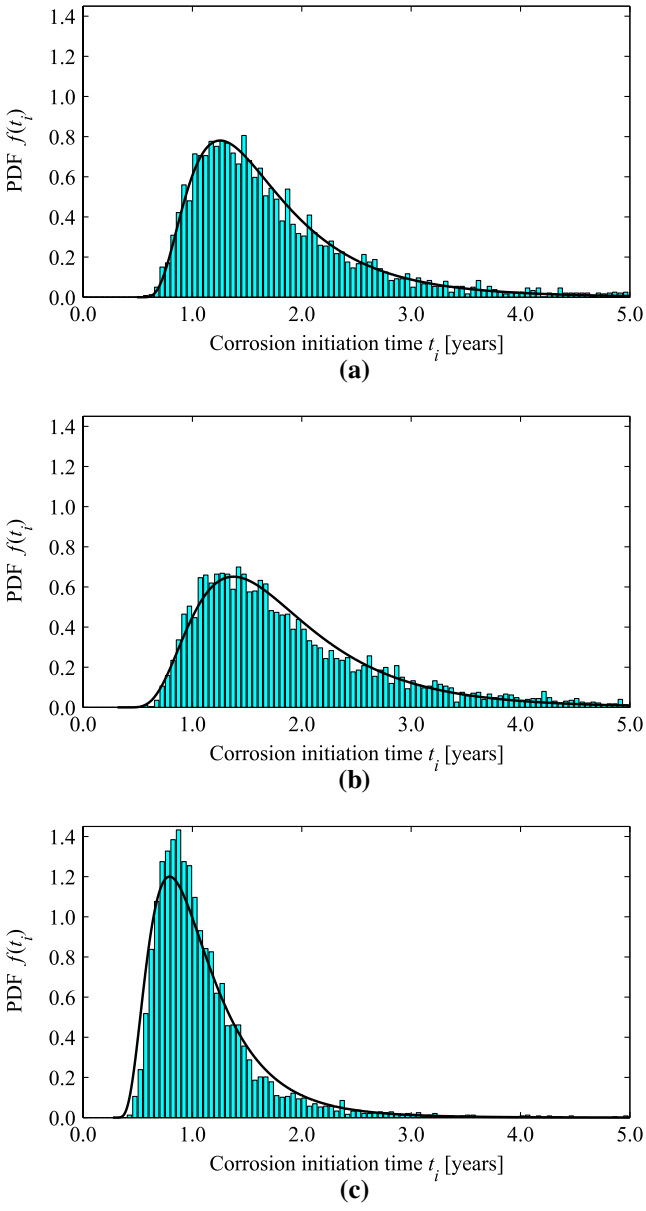

Figure 23. Probability mass function and lognormal probability density distribution model of the corrosion initiation time t_i of the steel bar #1 of the solid RC cross-section: (a) 1D diffusion; 2D diffusion from (b) one side ($\alpha = 0$), and (c) four sides ($\alpha = 1$).

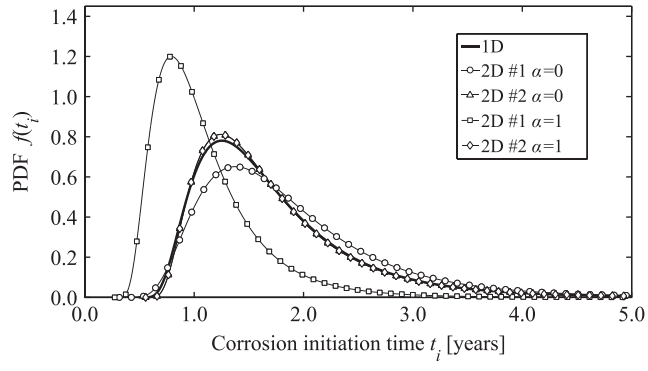

Figure 24. Comparison of the lognormal probability density distributions of the corrosion initiation time t_i of the steel bars #1 and #2 of the solid RC cross-section under 1D diffusion and 2D diffusion from one side ($\alpha = 0$) and four sides ($\alpha = 1$).

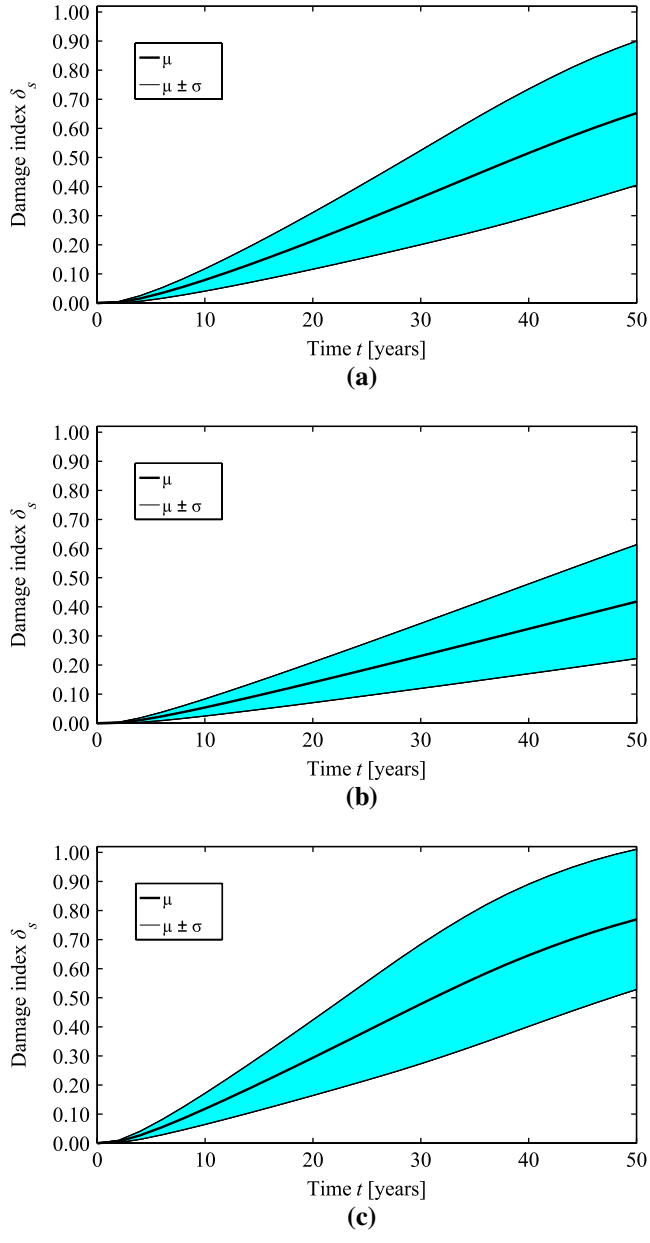

Figure 25. Evolution over time of the probabilistic parameters (mean μ and standard deviation σ) of the damage index δ_s of the steel bar #1 of the solid RC cross-section: (a) 1D diffusion; 2D diffusion from (b) one side ($\alpha = 0$), and (c) four sides ($\alpha = 1$).

is of interest to compare the accuracy of life-cycle predictions based on 1D and 2D diffusion models also in probabilistic terms. To this purpose, the results of probabilistic life-cycle analyses of the solid RC cross-section shown in Figure 17(a) are presented.

The probabilistic model considers the following quantities as random variables: concrete compression strength f_c; steel yielding strength f_{sy}; chloride content on the exposed surfaces C_0; diffusion coefficient D; steel damage rate coefficient q_s; critical chloride content C_{cr}. The nominal values of these quantities are assumed as mean values. The variables are considered uncorrelated with the probabilistic distribution and coefficients of variation listed in Table 2 (Biondini et al., 2006). The probabilistic analysis is carried out by Monte Carlo simulation and Latin Hypercube Sampling (Iman & Conover, 1982) with correlation control based on Simulated Annealing (Vořechovský & Novák, 2009). The termination criteria of the simulation

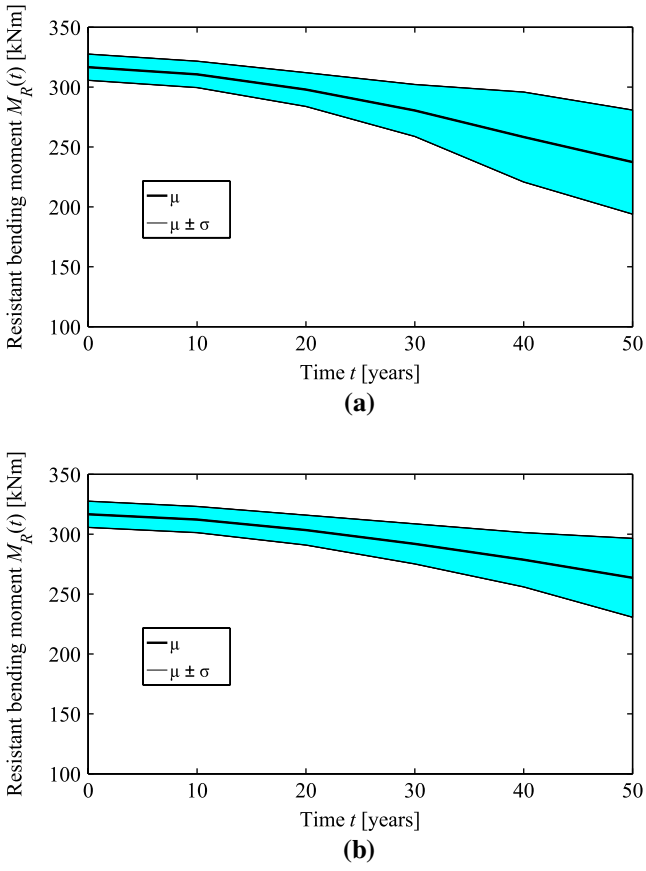

Figure 26. Evolution over time of the probabilistic parameters (mean μ and standard deviation σ) of the resistant bending moment M_R of the solid RC cross-section exposed on one side ($\alpha = 0$): (a) 1D diffusion; (b) 2D diffusion.

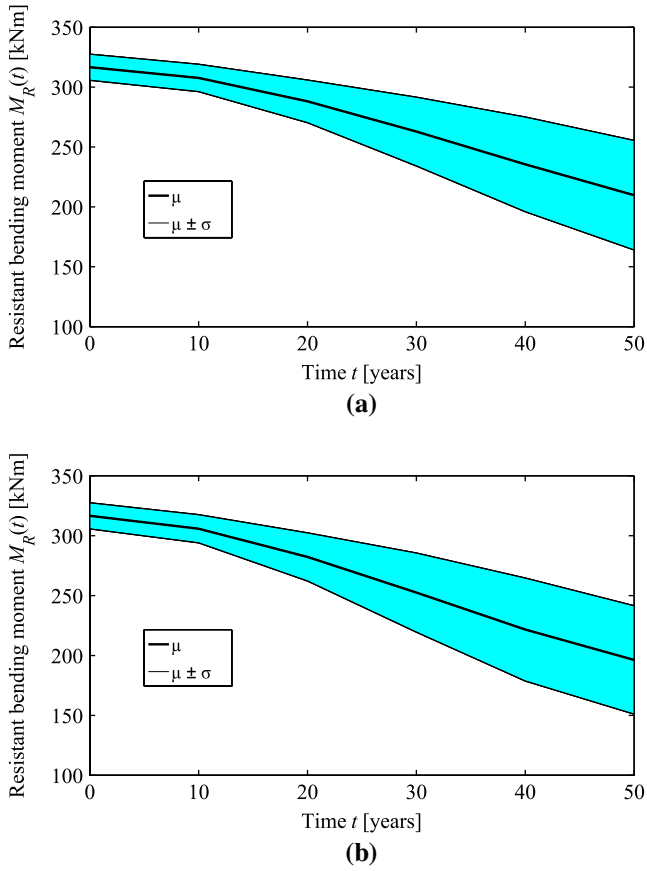

Figure 27. Evolution over time of the probabilistic parameters (mean μ and standard deviation σ) of the resistant bending moment M_R of the solid RC cross-section exposed on four sides ($\alpha = 1$): (a) 1D diffusion; (b) 2D diffusion.

process are based on a posteriori estimation of the goodness of the sample size based on a monitoring of the time-variant statistical parameters of the response random variables under investigation. Additional details about the simulation procedure can be found in Titi (2012).

Figure 23 shows the probability mass functions and the corresponding lognormal probability density distribution models of the corrosion initiation time t_i for the steel bar #1 of the RC cross-section under 1D diffusion (Figure 23(a)), 2D diffusion from one side (Figure 23(b)), and 2D diffusion from four sides (Figure 23(c)) based on a sample of 5000 Monte Carlo realisations. The three lognormal models have been referred to a minimum corrosion initiation time $t_{i,\min} = 0.49$, 0.32 and 0.27 years, respectively, computed to maximise the goodness of fit according to the Kolmogorov–Smirnov test.

In line with the results of the deterministic analysis, the comparison indicates that the corrosion initiation time computed using the 1D model tends to be underestimated for diffusion from one side, and overestimated for diffusion from four sides. For the case with full exposure, the 1D model leads to significant errors in terms of both mean value and dispersion measures. On the contrary, the error is negligible for the steel bar #2, as it is indicated by the comparison of the lognormal probability density distributions shown in Figure 24. However, significant errors may arise also for bar #2 if the corrosion starts at later stages of the diffusion process, as it may occur with larger values of concrete cover or under less severe exposures.

The influence of the diffusion modelling on the corrosion damage is described in Figure 25, which compares the evolution over time of the probabilistic parameters (mean μ and standard deviation σ) of the damage index δ_s of the steel bar #1 for the RC cross-section under 1D diffusion (Figure 25(a)), 2D diffusion from one side (Figure 25(b)), and 2D diffusion from four sides (Figure 25(c)). This comparison indicates that the 1D model can lead to significant errors in the assessment of the corrosion damage in terms of both mean value and dispersion measures, and that this error is generally higher than the error found for the corrosion initiation time. In fact, corrosion damage depends on both corrosion initiation and damage propagation.

Finally, Figures 26 and 27 illustrate the evolution over time of the probabilistic parameters of the resistant bending moment M_R of the RC cross-section subjected to positive bending under the two investigated exposure scenarios. These results confirm the inaccuracy of the 1D model, particularly in case of localised exposure, and indicates that a 2D model is necessary for an accurate assessment of the time-variant cross-sectional structural performance.

Conclusions

The main deterioration problem in concrete structures is the corrosion of reinforcement and related effects due to chloride attack. An accurate simulation of chloride diffusion and a proper modelling of the damage associated with corrosion are hence

essential for a reliable assessment of the lifetime performance of concrete structures in aggressive environment. Chloride ingress in concrete is generally modelled using the Fick's diffusion equation in the 1D form. However, in most cases the diffusion process should be more properly described by considering two- or three-dimensional patterns of concentration gradients.

In this paper, the accuracy of the 1D analytical modelling of diffusion and related damage has been investigated with respect to more accurate 2D formulations solved numerically using cellular automata. It has been found that the 1D analytical solution can provide accurate results only at the early stage of the diffusion process. Actually, the results of parametric analyses of the diffusion process for solid and hollow-core cross-sections showed that the 1D diffusion can lead over time to a significant loss of accuracy depending on the exposure conditions, the aspect ratio of the cross-section, the size of the openings and the location of points where the concentration and damage are evaluated. This loss of accuracy is also reflected in the assessment of corrosion damage of the reinforcing steel bars, as well as in the evaluation of the corresponding deterioration of cross-sectional performance indicators, such as bending strength and curvature ductility. Therefore, a 2D modelling of the diffusion process is generally required at cross-sectional level for an accurate life-cycle assessment of concrete structures exposed to corrosion.

This has been demonstrated both in deterministic and probabilistic terms by taking into account the uncertainty in material and geometrical properties and in the physical models of diffusion and damage processes. From the probabilistic investigation it has been found that both mean value and standard deviation of the corrosion initiation time computed using the 1D model tend to be underestimated for localised exposure, and overestimated for full exposure. Similar errors of the 1D model have been found in the corrosion propagation phase for the time-variant probabilistic parameters of both corroded area of steel bars and loss of cross-sectional bending strength, with significant overestimation for localised exposure and underestimation for full exposure.

The results of this investigation have clearly shown the primacy of general 2D numerical methods over simplified 1D analytical formulas. Such results have been achieved for pure chloride diffusion with constant diffusivity. Depending on the cracking patterns and in case of partially saturated concrete, for accurate results it may be necessary to consider additional factors in the 2D diffusion modelling, including multi-species diffusion under wetting/drying cycles, chloride ingress due to water sorption, chloride binding, time-variation of the diffusion coefficient and spatial variability of diffusivity associated with concrete cracking.

Disclosure statement

No potential conflict of interest was reported by the authors.

References

Al-Harthy, A.S., Stewart, M.G., & Mullard, J. (2011). Concrete cover cracking caused by steel reinforcement corrosion. *Magazine of Concrete Research, 63*, 655–667.

Almusallam, A.A. (2001). Effect of degree of corrosion on the properties of reinforcing steel bars. *Construction and Building Materials, 15*, 361–368.

Apostolopoulos, C.A., & Papadakis, V.G. (2008). Consequences of steel corrosion on the ductility properties of reinforcement bar. *Construction and Building Materials, 22*, 2316–2324.

Bastidas-Arteaga, E., Chateauneuf, A., Sánchez-Silva, M., Bressolette, Ph., & Schoefs, F. (2011). A comprehensive probabilistic model of chloride ingress in unsaturated concrete. *Engineering Structures, 33*, 720–730.

Bentz, D.P., Coveney, P.V., Garboczi, E.J., Kleyn, M.F., & Stutzman, P.E. (1994). Cellular automaton simulations of cement hydration and microstructure development. *Modelling and Simulation in Materials Science and Engineering, 2*, 783–808.

Bentz, D.P., Garboczi, E.J., Lu, Y., Martys, N., Sakulich, A.R., & Weiss, W.J. (2013). Modeling of the influence of transverse cracking on chloride penetration into concrete. *Cement and Concrete Composites, 38*, 65–74.

Bertolini, L. (2008). Steel corrosion and service life of reinforced concrete structures. *Structure and Infrastructure Engineering, 4*, 123–137.

Bertolini, L., Elsener, B., Pedeferri, P., & Polder, R. (2004). *Corrosion of steel in concrete*. Weinheim: Wiley-VCH.

Biondini, F. (2011). Cellular automata simulation of damage processes in concrete structures. Chapter 10. In: Y. Tsompanakis & B.H.V. Topping, (Eds.), *Soft computing methods for civil and structural engineering* (pp. 229–264). Stirlingshire: Saxe-Coburg.

Biondini, F., & Frangopol, D.M. (Eds.). (2008). *Life-cycle civil engineering*. Boca Raton, FL: CRC Press/Balkema, Taylor & Francis Group.

Biondini, F., & Frangopol, D.M. (2009). Lifetime reliability-based optimization of reinforced concrete cross-sections under corrosion. *Structural Safety, 31*, 483–489.

Biondini, F., & Nero, A. (2011). Cellular finite beam element for nonlinear analysis of concrete structures under fire. *Journal of Structural Engineering, 137*, 543–558.

Biondini, F., & Vergani, M. (2015). Deteriorating beam finite element for nonlinear analysis of concrete structures under corrosion. *Structure and Infrastructure Engineering, 11*, 519–532.

Biondini, F., Bontempi, F., Frangopol, D.M., & Malerba, P.G. (2004). Cellular automata approach to durability analysis of concrete structures in aggressive environments. *Journal of Structural Engineering, 130*, 1724–1737.

Biondini, F., Bontempi, F., Frangopol, D.M., & Malerba, P.G. (2006). Probabilistic service life assessment and maintenance planning of concrete structures. *Journal of Structural Engineering, 132*, 810–825.

Biondini, F., Camnasio, E., & Palermo, A. (2014). Lifetime seismic performance of concrete bridges exposed to corrosion. *Structure and Infrastructure Engineering, 10*, 880–900.

Biondini, F., Frangopol, D.M., & Malerba, P.G. (2008). Uncertainty effects on lifetime structural performance of cable-stayed bridges. *Probabilistic Engineering Mechanics, 23*, 509–522.

Bird, R.B., Stewart, W.E., & Lightfoot, E.N. (2002). *Transport phenomena* (2nd ed.). New York, NY: Wiley.

Boddy, A., Bentz, E., Thomas, M.D.A., & Hooton, R.D. (1999). An overview and sensitivity study of a multimechanistic chloride transport model. *Cement and Concrete Research, 29*, 827–837.

Cabrera, J.G. (1996). Deterioration of concrete due to reinforcement steel corrosion. *Cement and Concrete Composites, 18*, 47–59.

CEB. (1992). *Durable concrete structures – Design guide*. London: Thomas Telford.

Chen, S.-S., Frangopol, D.M., & Ang, A.-H.S. (Eds.). (2010). *Life-cycle of civil engineering systems*. Taipei: Taiwan Building Technology Center, DnE Information Service Net.

Cho, H.-N., Frangopol, D.M., & Ang, A.-H.S. (Eds.). (2007). *Life-cycle cost and performance of civil infrastructure systems*. London: Taylor & Francis Group, A.A. Balkema.

Crank, J. (1975). *The mathematics of diffusion*. Oxford: Clarendon Press.

Duprat, F. (2007). Reliability of RC beams under chloride-ingress. *Construction and Building Materials, 21*, 1605–1616.

Ellingwood, B.R. (2005). Risk-informed condition assessment of civil infrastructure: state of practice and research issues. *Structure and Infrastructure Engineering, 1*, 7–18.

Enright, M.P., & Frangopol, D.M. (1998). Probabilistic analysis of resistance degradation of reinforced concrete bridge beams under corrosion. *Engineering Structures, 20*, 960–971.

Estes, A.C., & Frangopol, D.M. (1999). Repair optimization of highway bridges using system reliability approach. *Journal of Structural Engineering, 125*, 766–775.

fib. (2006). *Model Code for service life design*. Bulletin 34. Fédération internationale du béton/International Federation for Structural Concrete, Lausanne, Switzerland.
Frangopol, D.M. (2011). Life-cycle performance, management, and optimization of structural systems under uncertainty: Accomplishments and challenges. *Structure and Infrastructure Engineering, 7*, 389–413.
Frangopol, D.M., & Furuta, H. (Eds.). (2001). *Life-cycle cost analysis and design of civil infrastructure systems*. Reston, VA: ASCE.
Frangopol, D.M., Kallen, M.-J., & van Noortwijk, J.M. (2004). Probabilistic models for life-cycle performance of deteriorating structures: Review and future directions. *Progress in Structural Engineering and Materials, 6*, 197–212.
Frangopol, D.M., Lin, K.-Y., & Estes, A.C. (1997). Reliability of reinforced concrete girders under corrosion attack. *Journal of Structural Engineering, 123*, 286–297.
Furuta, H., Frangopol, D.M., & Akiyama, M. (Eds.). (2014). *Life-cycle of structural systems: Design, assessment, maintenance and management*. London: CRC Press/Balkema, Taylor & Francis Group.
Garces Rodriguez, O., & Hooton, R.D. (2003). Influence of cracks on chloride ingress into concrete. *ACI Materials Journal, 100*, 120–126.
Glass, G.K., & Buenfeld, N.R. (2000). Chloride-induced corrosion of steel in concrete. *Progress in Structural Engineering and Materials, 2*, 448–458.
Glicksman, M.E. (2000). *Diffusion in solids*. New York, NY: Wiley.
Guzmán, S., Gálvez, J.C., & Sancho, J.M. (2011). Cover cracking of reinforced concrete due to rebar corrosion induced by chloride penetration. *Cement and Concrete Research, 41*, 893–902.
Hunkeler, F. (2005). Corrosion in reinforced concrete: processes and mechanisms. In: H. Böhni (Ed.), *Corrosion in reinforced concrete structures* (pp. 1–45). Cambridge: Woodhead.
Iman, R.L., & Conover, W.J. (1982). A distribution-free approach to inducing rank correlation among input variables. *Communications in Statistics – Simulation and Computation, 11*, 311–334.
Johannesson, B.F. (2003). A theoretical model describing diffusion of a mixture of different types of ions in pore solution of concrete coupled to moisture transport. *Cement and Concrete Research, 33*, 481–488.
Karaa, S., & Zhang, J. (2004). High order ADI method for solving unsteady convection–diffusion problems. *Journal of Computational Physics, 198*, 1–9.
Kilareski, W.P. (1980). Corrosion induced deterioration of reinforced concrete – An overview. *NACE Materials Performance, 19*, 48–50.
Mander, J.B., Priestley, M.J.N., & Park, R. (1988). Theoretical stress–strain model for confined concrete. *Journal of Structural Engineering, 114*, 1804–1826.
Margolus, N., & Toffoli, T. (1987). *Cellular automata machines. A new environment for modeling*. Cambridge, MA: MIT Press.
Medeiros, M.H.F., Gobbi, A., Réus, G.C., & Helene, P. (2013). Reinforced concrete in marine environment: Effect of wetting and drying cycles, height and positioning in relation to the sea shore. *Construction and Building Materials, 44*, 452–457.
Nielsen, E.P., & Geiker, M.R. (2003). Chloride diffusion in partially saturated cementitious material. *Cement and Concrete Research, 33*, 133–138.
Nowak, A.S., & Frangopol, D.M. (Eds.). (2005). *Advances in life-cycle cost analysis and design of civil infrastructure systems*. Lincoln, NE: University of Nebraska.
Papakonstantinou, K.G., & Shinozuka, M. (2013). Probabilistic model for steel corrosion in reinforced concrete structures of large dimensions considering crack effects. *Engineering Structures, 57*, 306–326.
Pastore, T., & Pedeferri, P. (1994). La corrosione e la protezione delle opere metalliche esposte all'atmosfera [Corrosion and protection of metallic structures exposed to the atmosphere]. L'edilizia, December 1994, 75–92 (In Italian).
Quarteroni, A., Sacco, R., & Saleri, F. (2007). *Numerical mathematics*. Berlin: Springer-Verlag.
Saetta, A.V., Schrefler, B.A., & Vitaliani, R.V. (1993). The carbonation of concrete and the mechanism of moisture, heat and carbon dioxide flow through porous materials. *Cement and Concrete Research, 23*, 761–772.
Schiff, J.L. (2008). *Cellular automata: A discrete view of the world*. Hoboken, NJ: Wiley.
Strauss, A., Frangopol, D.M., & Bergmeister, K. (Eds.). (2012). *Life-cycle and sustainability of civil infrastructure systems*. London: CRC Press/Balkema, Taylor & Francis Group.
Tang, L., & Gulikers, J. (2007). On the mathematics of time-dependent apparent chloride diffusion coefficient in concrete. *Cement and Concrete Research, 37*, 589–595.
Titi, A. (2012). *Lifetime probabilistic seismic assessment of multistory precast buildings* (PhD dissertation). Politecnico di Milano, Milan, Italy.
Titi, A., & Biondini, F. (2012). Validation of diffusion models for life-cycle assessment of concrete structures. In: A. Strauss, D.M. Frangopol, & K. Bergmeister (Eds.), *Life-cycle and sustainability of civil infrastructure systems*. Third International Symposium on Life-Cycle Civil Engineering (IALCCE 2012), Vienna, Austria, October 3–6. London: CRC Press/Balkema, Taylor & Francis Group.
Vick, B. (2007). Multi-physics modeling using cellular automata. *Complex Systems, 17*, 65–78.
Vidal, T., Castel, A., & François, R. (2004). Analyzing crack width to predict corrosion in reinforced concrete. *Cement and Concrete Research, 34*, 165–174.
Vořechovská, D., Podroužek, J., Chromá, M., Rovnaníková, P., & Teplý, B. (2009). Modeling of chloride concentration effect on reinforcement corrosion. *Computer-Aided Civil and Infrastructure Engineering, 24*, 446–458.
Vořechovský, M., & Novák, D. (2009). Correlation control in small-sample Monte Carlo type simulations I: A simulated annealing approach. *Probabilistic Engineering Mechanics, 24*, 452–462.
von Neumann, J. (1966). *Theory of self-reproducing automata*. Champaign, IL: University of Illinois Press.
Vu, K.A.T., & Stewart, M.G. (2000). Structural reliability of concrete bridges including improved chloride-induced corrosion models. *Structural Safety, 22*, 313–333.
Wolfram, S. (1994). *Cellular automata and complexity: Collected papers*. Boston, MA: Addison-Wesley.
Wolfram, S. (2002). *A new kind of science*. Champaign, IL: Wolfram Media.
Xi, Y., & Bažant, Z.P. (1999). Modeling chloride penetration in saturated concrete. *Journal of Materials in Civil Engineering, 11*, 58–65.
Xi, Y., Willam, K., & Frangopol, D.M. (2000). Multiscale modeling of interactive diffusion processes in concrete. *Journal of Engineering Mechanics, 126*, 258–265.
Yuan, Q., Shi, C., De Schutter, G., Audenaert, K., & Deng, D. (2009). Chloride binding of cement-based materials subjected to external chloride environment – A review. *Construction and Building Materials, 23*, 1–13.
Zhang, R., Castel, A., & François, R. (2010). Concrete cover cracking with reinforcement corrosion of RC beam during chloride-induced corrosion process. *Cement and Concrete Research, 40*, 415–425.